First-Principles Study of Casimir Repulsion in Metamaterials

Vassilios Yannopapas[1,2,*] and Nikolay V. Vitanov[2,3]

[1]*Department of Materials Science, University of Patras, GR-26504 Patras, Greece*
[2]*Department of Physics, Sofia University, James Bourchier 5 Boulevard, 1164 Sofia, Bulgaria*
[3]*Institute of Solid State Physics, Bulgarian Academy of Sciences, Tsarigradsko chaussée 72, 1784 Sofia, Bulgaria*
(Received 23 January 2009; published 17 September 2009)

We examine theoretically the Casimir effect between a metallic plate and several types of magnetic metamaterials in pursuit of Casimir repulsion, by employing a rigorous multiple-scattering theory for the Casimir effect. We first examine metamaterials in the form of two-dimensional lattices of inherently nonmagnetic spheres such as spheres made from materials possessing phonon-polariton and exciton-polariton resonances. Although such systems are magnetically active in infrared and optical regimes, the force between finite slabs of these materials and metallic slabs is plainly attractive since the effective electric permittivity is larger than the magnetic permeability for the studied spectrum. When lattices of magnetic spheres made from superparamagnetic composites are employed, we achieve not only Casimir repulsion but almost total suppression of the Casimir effect itself in the micrometer scale.

DOI: 10.1103/PhysRevLett.103.120401 PACS numbers: 03.70.+k, 12.20.−m, 42.50.Lc, 42.50.Nn

The Casimir force between two adjacent conducting surfaces [1] is of quantum nature as it arises from the exchange of virtual photons between the two surfaces, i.e., from the net momentum exchange of zero-point vacuum fluctuations confined between the surfaces. The theory for the Casimir force between two planar slabs of arbitrary material, in thermal equilibrium, has been provided by Lifshitz [2] and, almost always, results in an attractive force. Casimir forces manifest themselves in micro- and nanoscale devices such as micro- and nanoelectromechanical systems (MEMS and NEMS, respectively) which contain planar objects with large values of surface-to-volume ratio. In these systems, the Casimir forces cause individual parts in MEMS and NEMS to attract, slide, and/or stick together, resulting in failure of the device. It is, therefore, of paramount technological importance to design material structures for the control and manipulation of Casimir forces in MEMS/NEMS. The neutralization of Casimir forces by surface repulsion at short distances followed by attraction at larger distances has been the holy grail of macroscopic QED.

According to Lifshitz theory, a repulsive force arises when the surfaces have different electric permittivities ϵ and the medium between them possesses a permittivity in between the values of the two slabs [3]. Usually this situation corresponds to the case where the space between the two slabs is filled with a liquid. Based on this, a recent experiment has confirmed the existence of repulsive force between a gold sphere and a silica surface immersed in bromobenzene liquid [4].

A repulsive Casimir force may also arise between a ‘‘mostly electric’’ and a ‘‘mostly magnetic’’ slab [5], i.e., between a slab with $\epsilon > \mu$ and one with $\epsilon < \mu$, where μ is the magnetic permeability. The differences in ϵ and μ should be significant within the near infrared and/or visible regions in order to have a countable contribution to the net Casimir force. However, the response of naturally occurring ferromagnetic materials usually lies from the kHz up to the GHz regime. In this respect, there have been theoretical proposals based on effective-medium approximations claiming that such a situation is possible between a metallic slab (mostly electric) and a mostly magnetic metamaterial [6,7]. The latter are subwavelength artificial structures mimicking a homogeneous medium and designed to possess a desired electromagnetic feature such as resonances in the magnetic permeability within a given spectral region.

Based on an effective-medium description, it was suggested [8] that the use of a magnetic metamaterial without a Drude-type response in the long-wavelength limit, e.g., a metamaterial with polaritonic constituents, can induce a repulsive force to a metallic plate. However, the same authors in a more recent work [9] claimed that this was not feasible due to the trivial values of the effective magnetic permeability in the imaginary-frequency domain. In order to provide a definite answer to the above issue, one has to depart from the effective-medium approach and classical Lifshitz theory for homogeneous plates and resort to contemporary electromagnetic solvers which solve exactly Maxwell's equations and describe accurately the zero-point vacuum fluctuations [10–13]. In this Letter, by employing a rigorous multiple-scattering approach we show that the prediction of the effective-medium theory is correct and, indeed, slabs of polaritonic materials are not expected to exhibit a repulsive Casimir effect. However, using the same approach we show that metamaterials of spheres made from superparamagnetic nanocomposites result in total cancellation of the Casimir effect in the micrometer scale while, at the same time, exhibiting Casimir repulsion for small distances.

The zero-temperature Casimir interaction energy for two slabs of inhomogeneous metamaterials corresponding to the same two-dimensional (2D) periodic lattice is provided by the generalization of the corresponding formula for two homogeneous slabs [9]

$$E/S_0 = \hbar \int_0^\infty \frac{d\xi}{2\pi} \int_{\mathrm{SBZ}} \frac{d^2\mathbf{k}_\parallel}{(2\pi)^2} \ln\det[1 - \mathbf{R}_1\mathbf{R}_2]_{\{p\mathbf{g}\}}, \quad (1)$$

where $\mathbf{R}_1$ and $\mathbf{R}_2$ are the reflection matrices for each one of the two Casimir components which may be either a homogeneous slab or a finite slab of a metamaterial. In the matrix notation $\{p\mathbf{g}\}$, the symbol $\mathbf{g}$ stands for the reciprocal-lattice vectors associated with the given 2D lattice and $p = 1, 2$ refers to the two different polarization states of the electromagnetic field. $\mathbf{R}_1$ and $\mathbf{R}_2$ are calculated on the basis of a rigorous layer-multiple-scattering theory [14,15]. The phase factors representing the multiple-scattering events between the two slabs are incorporated within the definitions of $\mathbf{R}_1$ and $\mathbf{R}_2$ [14]. The $\mathbf{k}_\parallel$ integration in Eq. (1) is performed within the surface Brillouin zone (SBZ) of area S_0 associated with a given 2D lattice. The spectral integration in Eq. (1) is done for imaginary frequencies $\omega = i\xi$ provided that ϵ and μ contained therein are causal. The Casimir force F is given by the negative derivative of Eq. (1) with respect to the separation L between the two slabs. In the calculations that follow, the SBZ integration of Eq. (1) is performed by subdividing progressively the SBZ into smaller and smaller squares, within which a nine-point integration formula is very efficient. Using this formula we achieved excellent convergence with a total of 576 points in the SBZ. Also, the inclusion of 12 reciprocal-lattice $\mathbf{g}$-vectors in the matrix representation of $\mathbf{R}_1$ and $\mathbf{R}_2$ provided convergent results. Finally, since the frequency integration is performed along the imaginary axis, the lattice sums contained in matrices $\mathbf{R}_1$ and $\mathbf{R}_2$ are performed by summation in direct space since Ewald-summation schemes do not converge [14].

The layer-multiple-scattering method which provides the matrices $\mathbf{R}_1$ and $\mathbf{R}_2$ in Eq. (1) provides the transmission, reflection, and absorption coefficients of an electromagnetic wave incident on a composite slab consisting of a number of layers which can be either planes of nonoverlapping particles with the same 2D periodicity or homogeneous plates. For each plane of particles, the method calculates the full multipole expansion of the total multiply scattered wave field and deduces the corresponding transmission and reflection matrices in the plane-wave basis.

First, we calculate the Casimir force between a metallic slab and 2D square array of polaritonic spheres, i.e., spheres made from materials supporting polaritonic excitations. In these arrays the effective permeability μ_{eff} assumes nontrivial values [much larger or much smaller (even negative) than unity] in the infrared [16–18] and visible regimes [19,20].

We begin our study with the case of a square array of microspheres made from $LiTaO_3$. $LiTaO_3$ is an ionic material exhibiting phonon-polariton excitations [21], and as such, the corresponding electric permittivity has the form of a single-resonance Drude-Lorentz form, $\epsilon(\omega) = \epsilon_\infty[1 + (\omega_L^2 - \omega_T^2)/(\omega_T^2 - \omega^2 - i\omega\gamma)]$ where $\epsilon_\infty = 13.4$, $\gamma = 0.94 \times 10^{12}$ rad/sec. The respective $\omega_T = 26.7 \times 10^{12}$ rad/sec and $\omega_L = 46.9 \times 10^{12}$ rad/sec are the transverse and longitudinal optical phonon frequencies [22]. The period a of the square lattice is taken to be $a = c/\omega_T = 11.24$ μm and the radius of the spheres $S = 0.5c/\omega_T$; i.e., we deal with a close-packed array of spheres. The effective parameters ϵ_{eff} and μ_{eff} can be accurately calculated from the extended Maxwell-Garnett theory (EMG) [19,20,23,24].

The effective permeability μ_{eff} of the above structure exhibits strong resonant behavior in a spectral region below ω_T as shown in Fig. 1(a), owing to the large polarization currents induced by incident light at the Mie resonances of the individual spheres [17]. However, as seen from Fig. 1(a), the large values assumed by the $LiTaO_3$ permittivity introduce a strong resonance of ϵ_{eff} as well. For the case of the Casimir force, one actually needs the spectrum of μ_{eff} and ϵ_{eff} for imaginary frequencies as depicted in Fig. 1(b). Evidently, μ_{eff} assumes trivial values around unity in agreement with Ref. [9], and the metamaterial is mostly electric. Therefore, a repulsive Casimir force is not anticipated when a finite slab of the above polaritonic crystal is placed next to a metallic slab.

In order to confirm the above we have considered the setup of Fig. 2: a single plane of the above $LiTaO_3$ spheres is placed next to a gold plate. The permittivity of gold is provided by the Drude formula, i.e., $\epsilon(\omega) = 1 - \omega_p/[\omega(\omega + i\omega\tau^{-1})]$ with $\hbar\omega_p = 3.71$ eV and $(\omega_p\tau) = 20$. Figure 3(a) shows the Casimir force per unit area [negative derivative of Eq. (1)] for the above setup, normalized to the value of the classical Casimir force F_C between two perfect conductors: $F_C = -\hbar c\pi^2/(240L^4)$. The force is clearly attractive but much weaker than F_C. At the same time, it drops more slowly with L compared to F_C since the ratio F/F_C increases with L.

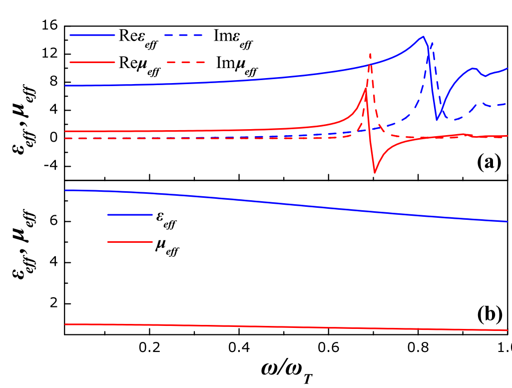

FIG. 1 (color online). Effective permeability μ_{eff} and permittivity ϵ_{eff} of a crystal of close-packed $LiTaO_3$ spheres with radius $S = 0.5c/\omega_T = 5.62$ μm for (a) real and (b) imaginary frequencies, as calculated by the EMG theory.

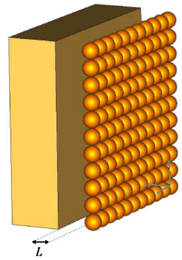

FIG. 2 (color online). Computational setup for Figs. 3 and 4: a square lattice of close-packed spheres placed opposite to a metallic slab. The distance between the slab and the surface of a sphere is denoted by L.

A similar picture is obtained for a nanosized array of CuCl spheres. CuCl is a semiconductor which possesses a strong Z_3 exciton line at 386.93 nm [25]. Around the exciton frequencies, the dielectric function of the CuCl is given by $\epsilon_s(\omega) = \epsilon_\infty + A\gamma/(\omega_0 - \omega - i\gamma)$, where $A = 632$ and it is proportional to the exciton oscillation strength. The rest of the parameters for CuCl are [25] $\epsilon_\infty = 5.59$, $\hbar\omega_0 = 3.363$ eV, and $\hbar\gamma = 5 \times 10^{-5}$ eV. Figure 3(b) shows the normalized Casimir force F/F_C for a 2D array of close-packed CuCl nanospheres of radius $S = c/\omega_0 = 29.4$ nm in the setup of Fig. 2. This time, the separation L is of the order of nanometers. Again, the Casimir force is attractive, it decays more slowly than F_C, and it is 2 orders of magnitude weaker than F_C. We expect that a similar picture holds for other polaritonic metamaterials, either in the infrared (e.g., SiC, TlBr, TlCl) or visible regimes (e.g., Cu_2O).

The agreement between the EMG theory and the rigorous approach based on Eq. (1) is due to the integration over

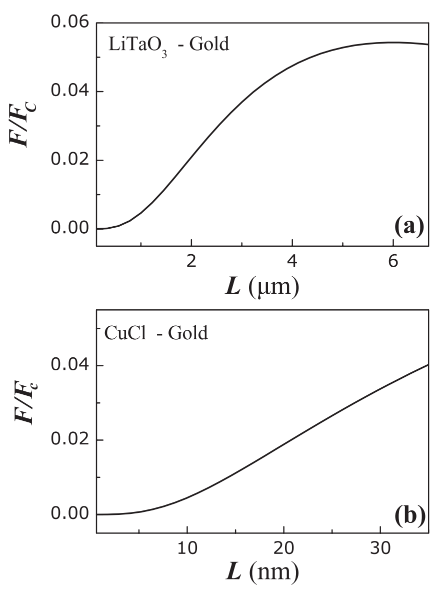

FIG. 3. Normalized Casimir force F/F_C for the setup of Fig. 2 where the square lattice consists of (a) close-packed $LiTaO_3$ spheres of radius $S = 5.62\ \mu$m, and (b) close-packed CuCl spheres of radius $S = 29.4$ nm.

imaginary frequencies $i\xi$ which makes all wave components evanescent with rate $k_z = \sqrt{(\xi/c)^2 + (\mathbf{k}_\parallel + \mathbf{g})^2}$. Waves close to the center of the SBZ, i.e., $\mathbf{k}_\parallel \to 0$, are those which dominate the Casimir effect; however, the limit $\mathbf{k}_\parallel \to 0$ (long-wavelength limit) is the region of validity of effective-medium theories such as the EMG theory considered here.

In pursuit of a purely magnetic system which would provide Casimir repulsion together with a metallic slab, an obvious choice would be naturally occurring ferromagnetic materials. Unfortunately, these exhibit a magnetic response far below the infrared and optical regimes as is required for the Casimir effect. However, very small nanoparticles of ferromagnetic materials become superparamagnetic in the infrared regime due to the drastic reduction of the relaxation time τ needed for the (permanent) magnetic dipoles to align parallel to an applied magnetic field. We therefore consider a composite material consisting of 3 nm Ni nanoparticles embedded in an insulating matrix such as Al_2O_3. By extending Onsager's theory, it can be shown [26] that such a nanocomposite material exhibits superparamagnetic behavior in the infrared regime. Since alignment of the magnetic dipoles in Ni is analogous to the alignment of (permanent) electric dipoles in an insulator under an external electric field, the permeability μ_c calculated in Ref. [26] was fitted by a Debye relaxation model, i.e., $\mu_c(\omega) = \mu_\infty + \Delta/(1 - i\omega\tau_c)$ with $\mu_\infty = 0.733$, $\Delta = 9.98$, and $\tau_c^{-1} = 1.78 \times 10^{12}\ \mathrm{sec}^{-1}$. The corresponding permittivity ϵ_c is provided by the Clausius-Mossoti formula, $\epsilon_c(\omega) = \epsilon_{Al_2O_3}[(1 + 2f)\epsilon_{Ni} + 2(1 - f)\epsilon_{Al_2O_3}]/[(1 - f)\epsilon_{Ni} + (2 + f)\epsilon_{Al_2O_3}]$, where ϵ_{Ni}, $\epsilon_{Al_2O_3}$ are the permittivities of Ni and Al_2O_3, respectively, and f is the volume filling fraction occupied by the Ni nanospheres and is taken as $f = 0.2$ [27]. We note that instead of the Clausius-Mossoti formula, one can equally make use of the EMG theory and obtain the same results for ϵ_c.

We consider a square lattice of microspheres ($S = 84\ \mu$m) made from the above nanocomposite [Ni-Al_2O_3, see Fig. 4(a)] and optical properties described by μ_c, ϵ_c given above. The Ni-Al_2O_3 microspheres are arranged in a close-packed configuration as in Fig. 2. The imaginary-frequency spectra of the effective parameters ϵ_{eff}, μ_{eff} of the above lattice, as calculated by the EMG theory, are drawn in Fig. 4(b). It is evident that μ_{eff} is much larger than ϵ_{eff} for a wide range of frequencies promising the emergence of repulsive Casimir forces. Indeed, by observing the solid line of Fig. 4(c), we see that the Casimir force becomes repulsive for distances $L < 16\ \mu$m. Moreover, although it is not clear from the broken line of Fig. 4(b) (log scale is needed), the most striking result of Fig. 4(b) is the fact that the ratio F/F_C becomes very small (e.g., for $L \simeq 1\ \mu$m, $F/F_C \sim 10^{-8}$) suggesting almost total suppression of the Casimir effect. In previous work where toy-model functions for ϵ_{eff} and μ_{eff} of the metamaterials have been employed [7–9], a Casimir repulsion appears at

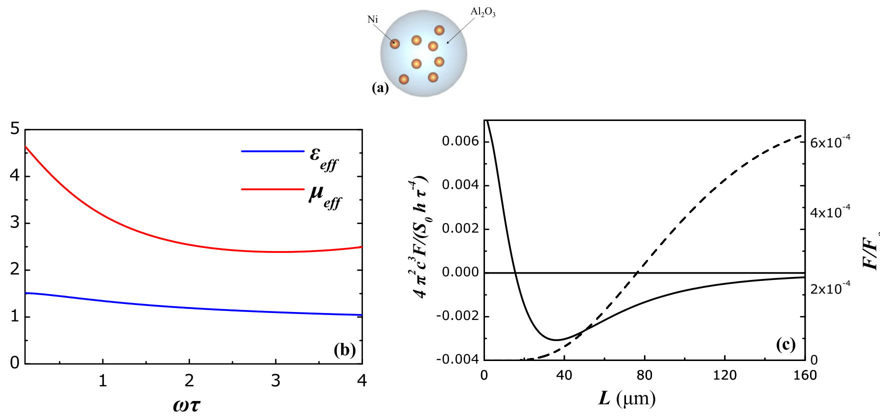

FIG. 4 (color online). (a) Microsphere made from a composite material of 3 nm Ni particles within an Al_2O_3 matrix with $f = 20\%$. (b) $\mu_{\rm eff}$ and $\epsilon_{\rm eff}$ for imaginary frequencies of a crystal of close-packed spheres of (a) with radius $S = 84$ μm, as calculated by the EMG theory. (c) Corresponding Casimir force in dimensionless units (solid curve—left axis) and normalized to F_C (broken curve—right axis).

intermediate and long separations between the metamaterial and the metallic slab while for short distances the Casimir force is attractive. Our *ab initio* results which indicate repulsive Casimir force at short distances ($L \rightarrow 0$) verify the prediction of Casimir repulsion at small separations occurring between a purely dielectric and a purely magnetic material [7,28]. Casimir repulsion at all distances has been also measured in Ref. [4].

In conclusion, on the basis of a rigorous electromagnetic multiple-scattering theory for imaginary frequencies, we have shown that Casimir repulsion cannot be achieved with metamaterials made from purely dielectric materials despite their magnetic activity in the desired frequency regions (infrared and optical). However, metamaterials of microspheres made from superparamagnetic nanocomposites embedded in an insulating matrix behave as mainly magnetic metamaterials and result in Casimir repulsion at short distances. Moreover, in the region of Casimir repulsion, the force values are also much suppressed compared to the ordinary Casimir effect, promising application in neutralizing quantum stiction in MEMS-based devices.

This work has been supported by the European Commission's projects EMALI and FASTQUAST, and the Bulgarian NSF Grants No. VU-F-205/06, No. VU-I-301/07, and No. D002- 90/08.

*vyannop@upatras.gr

[1] H. B. G. Casimir, Proc. K. Ned. Akad. Wet. **51**, 793 (1948).
[2] E. M. Lifshitz, Sov. Phys. JETP **2**, 73 (1956).
[3] I. E. Dzyaloshinskii, E. M. Lifshitz, and L. P. Pitaevskii, Adv. Phys. **10**, 165 (1961).
[4] J. N. Munday, F. Capasso, and V. A. Parsegian, Nature (London) **457**, 170 (2009).
[5] O. Kenneth *et al.*, Phys. Rev. Lett. **89**, 033001 (2002).
[6] C. Henkel and K. Joulain, Europhys. Lett. **72**, 929 (2005).
[7] I. G. Pirozhenko and A. Lambrecht, J. Phys. A **41**, 164 015 (2008).
[8] F. S. S. Rosa, D. A. R. Dalvit, and P. W. Milonni, Phys. Rev. Lett. **100**, 183602 (2008).
[9] F. S. S. Rosa, D. A. R. Dalvit, and P. W. Milonni, Phys. Rev. A **78**, 032117 (2008).
[10] V. Yannopapas and N. V. Vitanov, Phys. Rev. Lett. **99**, 120406 (2007).
[11] V. Yannopapas, Phys. Rev. B **76**, 235415 (2007).
[12] A. Rodriguez *et al.*, Phys. Rev. Lett. **99**, 080401 (2007).
[13] A. Rodriguez *et al.*, Phys. Rev. A **76**, 032106 (2007).
[14] N. Stefanou, V. Yannopapas, and A. Modinos, Comput. Phys. Commun. **113**, 49 (1998); **132**, 189 (2000).
[15] In Ref. [14], the reflection matrices $\mathbf{R}_1$ and $\mathbf{R}_2$ appear as $\mathbf{Q}^{\rm II}(1)$ and $\mathbf{Q}^{\rm III}(2)$, respectively.
[16] K. C. Huang, M. L. Povinelli, and J. D. Joannopoulos, Appl. Phys. Lett. **85**, 543 (2004).
[17] V. Yannopapas and A. Moroz, J. Phys. Condens. Matter **17**, 3717 (2005); V. Yannopapas, Phys. Rev. B **75**, 035112 (2007).
[18] M. S. Wheeler, J. S. Aitchison, and M. Mojahedi, Phys. Rev. B **72**, 193103 (2005).
[19] V. Yannopapas and N. V. Vitanov, Phys. Rev. B **74**, 193304 (2006).
[20] V. Yannopapas, J. Phys. Condens. Matter **20**, 255 201 (2008).
[21] C. Kittel, *Introduction to Solid State Physics* (Wiley, New York, 1976).
[22] M. Schall, H. Helm, and S. R. Keiding, Int. J. Infrared Millim. Waves **20**, 595 (1999).
[23] W. T. Doyle, Phys. Rev. B **39**, 9852 (1989).
[24] R. Ruppin, Opt. Commun. **182**, 273 (2000).
[25] M. Artoni, G. La Rocca, and F. Bassani, Phys. Rev. E **72**, 046604 (2005).
[26] P. Sheng and M. Gadenne, J. Phys. Condens. Matter **4**, 9735 (1992).
[27] M. Gadenne, in *Optical Properties of Nanostructured Random Media*, Topics Appl. Phys. Vol. 82 (Springer, Berlin, 2002), p. 249.
[28] T. Boyer, Phys. Rev. A **9**, 2078 (1974).